1   # PROPERTIES OF A TERNARY CALCIUM SULFOALUMINATE -

2   # CALCIUM SULFATE -FLY ASH CEMENT

3

4

5   SOCRATES IOANNOU[* a],   LUCIA REIG [b],   KEVIN PAINE [a],   KEITH QUILLIN[c]

6

7

8   a. University of Bath, Claverton Down, Bath, BA2 7AY, United Kingdom.

9   b. Universitat Jaume I. Avenida de Vicent Sos Baynat, s/n, 12006, Castellón de la Plana,   Spain

10   c. Building Research Establishment, Bucknalls Lane, Watford, WD25 9XX, United Kingdom.

11

12

13

14   * Corresponding author's address: Wolfson Centre for Materials Processing, Brunel University,

15   Kingston Lane, Uxbridge, UB8 3PH, London, United Kingdom

16   Email: Socrates.Ioannou@brunel.ac.uk

17   Tel: +44 (0) 7939983468

18   Fax: N/A

19

20

21

22

23 **Abstract**

24
25
26 In this paper, cement combinations based on calcium sulfoaluminate cement (CSAC) were

27 developed and the effect of fly ash and the hemihydrate form of calcium sulfate on the properties

28 of the systems were studied. Fly ash (FA), anhydrite (ANH), flue-gas desulfurization gypsum

29 (FGDG) and plaster gypsum (PL) were used to develop appropriate CSAC/calcium sulfate and

30 CSAC/calcium sulfate/addition systems, the hydration of which were studied. Tested properties of

31 cements were the compressive strength and the setting times. The results suggest that the use of fly

32 ash in the presence of anhydrite accelerates the formation of a strong ettringite-rich matrix that

33 firmly accommodated unreacted fly ash particles, both synergistically contributing to a dense

34 microstructure. At a given sulfate content, the use of anhydrite was shown to be favourable in

35 terms of the setting times, heat patterns and strength development compared to the hemihydrate-

36 based formulations.

37

38 **Keywords:**

39 D**.** Sulfoaluminate

40 D. Ettringite

41 D. Fly ash

42 Anhydrite

43 Hemihydrate

44

45 **Abbreviations:**

46 E=Ettringite

47 A=Anhydrite

48 Y=Ye'elimite

49   L=Gehlenite

50   Q=Quartz

51   S=Stratlingite

52   G= Gypsum

53   M=Mullite

54

55

56   **1. Introduction**

57

58

59   The blending of by-products and additions with Portland cement (PC) is a well established

60   approach to reducing the CO_2 emissions associated with the energy-intensive manufacture of

61   cement. Currently 3.3 billion tonnes of PC are globally manufactured every year and it is estimated

62   that the embodied CO_2 (eCO_2) for PC production is approximately 930kg of CO_2 per tonne of PC

63   produced [1, 2]. An alternative way to reduce the eCO_2 of concrete is through the use of non-PC

64   based systems as the binding ingredient. Calcium sulfoaluminate cements (CSAC), which have a

65   lower eCO_2 than PC, have been developed and used in China on an industrial scale since the 1970s

66   [3]. The primary raw materials are limestone, bauxite (or an aluminous clay) and gypsum, although

67   by-products such as fly ash may be also used [4]. The preparation of clinker is achieved by burning

68   the raw materials at temperatures in the range 1300-1350°C in rotary kilns. This is 100-150°C

69   lower than PC production and thus the energy input requirement is lower. Manufacturing process is

70   similar to that of PC although the resulting clinker has better grindability [5], leading to additional

71   savings of 15-30 kWh with respect to energy consumption [6]. By considering the eCO_2 emissions

72   of individual cement compounds as given in [7], it can be estimated that the eCO_2 of a typical pure

73   CSAC, consisting of ye'elimite, belite and aluminoferrite, is approximately 600 kg/t. This

74   represents a reduction in eCO_2 of approximately 35% when compared to PC.

75

76

77   The primary hydration product of CSAC is ettringite ($3CaO.Al_2O_3.3CaSO_4.32H_2O$) which forms at

78   early ages (less than 48 hours) as prismatic needles. Ettringite forms in the presence of sufficient

79   calcium sulfate (gypsum or anhydrite) which can be either blended with the ye'elimite-rich clinker

80   or added in the raw meal intergrinding process. The optimum amount of calcium sulfate for

81   dominant formation of ettringite depends on several parameters i.e. the ye'elimite content, the

82   calcium sulfate content and their respective molar ratios [8]. If there is deficiency in calcium

83   sulfate, then there is a tendency for monosulfoaluminate to form; whereas an excess of calcium

84   sulfate may lead to unstable expanding systems. Other products of the hydration of CSAC are

85   mainly aluminate hydrates, calcium silicate hydrates although unreacted ye'elimite is also typically

86   present. Strengths of CSAC-based cements may reach over 40MPa at 24 hours [9] and they have

87   been reported to exhibit very good resistance to aggressive environments, particularly to sulfate

88   environments [10, 11]. This is because aluminate-based phases are bound as sulfoaluminates at

89   early stages of hydration and these are not available for reaction with external sulfate agents to

90   form expansive ettringite.

91

92

93   The work reported in this paper aims to investigate the influence of two main aspects revolving

94   around the optimization of hydration and performance of CSAC-based cement systems. The first is

95   the form of calcium sulfate incorporated in the system recognising that the hemihydrate form is

96   more readily available than anhydrite. The second aspect covered the development of a ternary

97   system through the use of a low eCO_2 addition, particularly fly ash, which could provide a better

98   balance between performance and eCO_2.

99

100

101

1.1 The calcium sulfate source

103

There is a considerable experimental activity on CSAC that has been focusing on the use of anhydrite as the calcium sulfate source in the CSAC system. Extensive work throughout the last decades is encapsulated in review articles [12-13]. Indeed, consensus indicates that anhydrous calcium sulfate is the predominant and preferable calcium sulfate source within the system. The use of other forms of calcium sulfate, particularly hemihydrate, however, are not fully documented so as to offer justifications of any cost-based, environmental-based or performance-based advantages associated with anhydrite preference in CSAC. Moreover, such lack of available data does not provide a clear indication of the influence of the hemihydrate of calcium sulfate on the hydration of CSAC. A more detailed look is therefore required at this type of calcium sulfate.
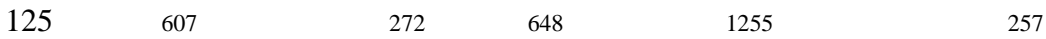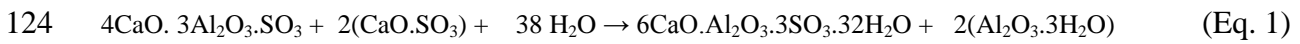
113

114

The intrinsic properties of both hemihydrate calcium sulfate and anhydrite are compared and established [14-15]. Setting times of the hemihydrate are known to be considerably short due to its high solubility (typically in the range of 7-9 g/l) and its reactivity, as opposed to that of anhydrite (approximately 2.5.-3.0 g/l) [16]. Equations 1 and 2 suggest that during the reaction of both calcium sulfate forms with ye'elimite, the quantities of ettringite and $Al(OH)_3$ formed are comparable. The only changing parameter is the amount of water needed for complete phase formation.

122

123 Ye'elemite + Anhydrite:
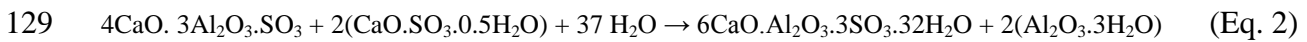
124 $4CaO. 3Al_2O_3.SO_3 + 2(CaO.SO_3) + 38 H_2O \rightarrow 6CaO.Al_2O_3.3SO_3.32H_2O + 2(Al_2O_3.3H_2O)$ (Eq. 1)

125   607   272   648   1255   257

126

127

128 Ye'elemite + Hemihydrate:

129 $4CaO. 3Al_2O_3.SO_3 + 2(CaO.SO_3.0.5H_2O) + 37 H_2O \rightarrow 6CaO.Al_2O_3.3SO_3.32H_2O + 2(Al_2O_3.3H_2O)$ (Eq. 2)

130   607   290   666   1255   257

131

132

133

134 Based on the available literature and data, it is therefore necessary to distinguish the beneficial

135 characteristics offered by each form of calcium sulfate when incorporated in a CSAC system.

136

137

138 *1.2 The use of fly ash in CSAC/calcium sulfate system*

139

140

141 Although the eCO_2 associated with the use of an optimized CSAC/calcium sulfate system may be

142 lower than that of PC, potentially greater savings may be achieved based on the development of

143 ternary CSAC-based systems with maintained performance properties.

144

145 By-products from coal combustion plants are associated with almost zero eCO_2, whilst they may

146 provide microstructural and mechanical advantages to cementitious systems when incorporated at

147 optimum percentages. One advantage is the pozzolanic reaction. The use of low eCO_2 pozzolanic

148 by-products- particularly fly ash- in the CSAC system, may instigate reaction with $Ca(OH)_2$

149 yielding from belite hydration in CSAC thus providing additional C-S-H gel. Previous studies on

150 compressive strengths of CSAC/fly ash blends suggest a slight decrease in strengths when fly ash

151 contents are higher than 10% [17]. However, there is still limited understanding and lack of data on

152 the hydration mechanisms of such systems. Given this, and by considering the advantageous effect

153 of particle packing that fly ash may potentially provide when acting as a low-eCO$_2$ filler, then it is

154 possible that a more sustainable system may be developed while maintaining its mechanical and

155 microstructural properties.

156
157

158 **2. Materials and methods**

159
160
161 The materials used in this study are shown in Table 1. Particle size distribution was determined

162 using a Malvern Mastersizer 2000 laser diffraction equipment. Anhydrite (ANH), plaster (PL) and

163 flue gas desulphurization gypsum (FGDG), were used as the calcium sulfate sources in the CSAC

164 system.

165   *Table 1. Materials used in the experimental*

Material	Abbreviation	Particle density (kg/m^3)	Mean diameter size (μm)	Particle size distribution (μm)	
				d$_{10}$	d$_{90}$
Calcium sulfoaluminate cement	CSAC	2790	25.3	2.2	64.8
Fly ash, category N to BS EN 450-1:2012 [18]	FA	2290	34.5	2.4	81.6
Calcium sulfate: Flue gas desulfurization gypsum	FGDG	2520	47.4	8.7	119.2
Calcium sulfate : Gypsum plaster	PL	2600	27.5	3.2	86.2
Calcium sulfate : Anhydrite	ANH	2950	24.5	2.3	42.1

166

167 The ye'elimite content in the CSAC clinker was found to be 71% and the belite content was 15%,

168 although no calcium sulfate was detected. To confirm the sulfate type in FGDG, PL, and ANH, TG

169 analysis (20°C to 300°C at a rate of 10°C/min) was conducted and mass losses of 5.43% and 5.16%

170 respectively were obtained in the range of 135-137°C. No mass loss was observed in ANH.

171

172

173 In order to assess the hydration processes of the systems, cement pastes were prepared at a w/c

174 ratio of 0.5 and cured in a 20°C water-curing tank until age of testing. TG and XRD analyses were

175 performed after 1, 3, 7 and 28 curing days and SEM images of the pastes cured for 28 days were

176 obtained, assuming that this period was adequate for allowing full formation of all hydration

177 products. Acetone was used to arrest the hydration of the cements.

178 Setting times of the pastes were determined in accordance to BS EN 196-3:1995 [19]. Heat of

179 hydration was determined using a Wexham developments JAF conduction calorimeter. Mortar

180 samples were prepared to assess the mechanical properties and dimensional changes of the

181 combinations. The compressive strength was conducted in accordance to BS EN 196-1:1995 [20]

182 and the dimensional changes were monitored on air-cured mortar samples stored in conditioning

183 chamber (maintained 20°C, 65% RH) at 1, 7, 28 and 90 days of age.

184

185

186 For the development of appropriate CSAC/calcium sulfate combinations, the following criteria

187 were taken into consideration:

188

189

190 • Achievement of a cement strength class equivalent (or higher) to that of a 42,5N (or R)

191 conventional cement as defined in BS EN 197-1:2000 [21]

192 • A calcium sulfate content lower than that which creates dimensional instability. This was

193 achieved experimentally by monitoring the dimensional change of CSAC/calcium sulfate cement

194 pastes at increasing calcium sulfate contents.

195

196

197 • A minimum content of calcium sulfate in the system to ensure ettringite formation and

198 avoid monosulfoaluminate formation by using stoicheiometric approach.

199

200

201 To examine the influence of the type and amount of the calcium sulfate sources on the mechanical

202 properties and dimensional stability of the system, combinations were prepared at varying calcium

203 sulfate contents, i.e. CSAC/calcium sulfate: 100/0, 80/20; 65/35; 50/50; 35/65 as shown in Table 2.

204

205

206 For the development and selection of appropriate CSAC/anhydrite/FA combinations (denoted as

207 GAF in Table 2), FA was introduced at contents of 5%, 10% and 15% by mass of total

208 combination, whilst maintaining the CSAC/anhydrite ratio that satisfied all criteria previously

209 stated. The particular percentage range of FA was selected based on determining approximately the

210 minimum amount of $Ca(OH)_2$ likely to be formed from belite hydration so as to promote

211 pozzolanic reaction.

212

213

214 To establish the minimum calcium sulfate content for sufficient ettringite formation, a

215 stoicheiometric approach was used. For complete ettringite formation in both cases, the molecular

216 mass ratios of calcium sulfate to ye'elimite needed to be considered based on equations 1 and 2.

217   The ratios were determined as 290/607=0.477 and 272/607= 0.448 for hemihydrate and anhydrite

218   respectively. Based on the chemical composition of the as-received high-strength CSAC, the pure

219   ye'elimite content was 71% and no calcium sulfate was added and/or interground in advance during

220   manufacturing. It was assumed that the full amounts of added calcium sulfate reacted solely with

221   ye'elimite, therefore, the minimum calcium sulfate content required to promote ettringite formation

222   and avoid monosulfoaluminate formation was calculated as 0.477x0.71 ≈ 34% for the hemihydrate

223   and 0.448 x 0.71 ≈ 32% for the anhydrite respectively. The two contents were then considered as

224   the limits for defining chemically stable CSAC/ANH and CSAC/hemihydrate combinations.

225

226

227
<p align="center">Table 2. Mix proportions and compressive strength development of combinations used</p>

Cement / Combination	Notation	CSAC	FGDG	PL	ANH	FA	Compressive strength N/mm² at day				
							1	3	7	28	90
CSAC		100	-	-	-	-	36.2	43.7	57.4	76.1	72.2
CSAC/FGDG	FGDG1	35	65	-	-	-	6.8	8.1	9.4	16.3	10.2
	FGDG2	50	50	-	-	-	14.3	18.1	19.9	32.3	30.7
	FGDG3	65	35	-	-	-	24.0	31.8	37.6	42.7	46.9
	FGDG4	80	20	-	-	-	28.2	36.6	45.9	61.0	62.1
CSAC/ANH	ANH1	35	-	-	65	-	4.2	6.3	9.1	11.6	11.5
	ANH2	50	-	-	50	-	11.9	21.9	25.8	43.3	47.1
	ANH3	65	-	-	35	-	22.9	29.0	39.5	46.0	49.7
	ANH4	80	-	-	20	-	31.9	39.4	50.0	67.1	67.2
CSAC/PL[1]	PL1/2/3	80/65/50	-	20/35/50	-	-	-	-	-	-	-
CSAC/ANH/FA	GAF5	61	-	-	34	5	29.3	37.8	39.7	51.1	51.2
	GAF10	58	-	-	32	10	30.8	36.2	39.2	49.6	49.4
	GAF15	55	-	-	30	15	31.5	35.1	38.9	48.8	48.2

228

229

230

231

232

---

[1] The preparation and study of CSAC/PL-based mortars in certain techniques was not possible because of the rapid setting that occurred.

233 **3. Results and discussion**

234

235

236 *3.1. Dimensional stability*

237

238

239 Dimensional changes of CSAC/ANH and CSAC/FGDG mortars at varying contents of calcium

240 sulfate are shown in Figures 1 and 2 respectively. Due to rapid setting that occurred in CSAC/PL

241 combinations, preparation and tests were not possible. It can be seen that at calcium sulfate

242 contents below 50%, both FGDG and ANH-based formulations exhibited similar and almost

243 dimensionally neutral patterns at early ages. These were followed by a slight shrinkage on the

244 region of $5\text{-}10\text{x}10^{-4}$ on the 28th day, reaching the maximum values on the 90th day. When calcium

245 sulfate contents reached above 50%, expansion occurred to both combinations with severe cracks

246 forming at a sulfate content of 65% which is a characteristic of ettringite's instability when

247 ye'elimite is introduced in exceedingly high sulfate concentrations. Based on these results, the

248 value of 50% was considered as the maximum content when selecting stable CSAC/calcium sulfate

249 combinations. Shrinkage patterns of CSAC/FGDG were less than those observed CSAC/ANH at a

250 given proportion, with a difference ranging from approximately 50 to $180\text{x}10^{-4}$ strains. This was

251 because, for the two calcium sulfate types to yield the same molecular weight of ettringite upon

252 their reaction with ye'elimite, the hemihydrate content requirement was higher than that of

253 anhydrite, according to Equation 2 and Figure 3. Towards the 90th day of examination, slight

254 shrinkage was observed at both CSAC/ANH and CSAC/FGDG samples at calcium sulfate contents

255 less than 50%, probably due to a small degree of ongoing water evaporation occurred after

256 complete ettringite formation.

257

258

259 *3.2. Compressive strength development*

260

261

262 Compressive strength development of water-cured CSAC/FGDG, CSAC/ANH and GAF mortars

263 at increasing calcium sulfate contents are shown in Table 2.

264

265 For the CSAC/calcium sulfate combinations the results show that, regardless of the calcium sulfate

266 type introduced, the compressive strength values tend to decrease at increasing ANH or FGDG

267 contents. Highest strengths were observed in pure CSAC mortars. This is in coherence with

268 previous work [22] when considering 7-day and 28-day values. During the first 24 hours of

269 hydration, the formation of ettringite in the CSAC/calcium sulfate systems would be mainly

270 responsible for the systems' strength development as evidenced from TG, XRD and SEM analyses

271 in Figures 4-11. In pure CSAC, where the ye'elimite content is highest compared to all other

272 formulations, the strength evolution at very early ages would be dependent on the formation of

273 other hydration products, most probably C-A-H, $Al(OH)_3$ and little amounts of ettringite due to

274 absence of calcium sulfate. The effect of this possible set of hydration products on the strength

275 development of pure CSAC could potentially be greater than that of ettringite upon the

276 CSAC/calcium sulfate systems. This is because, according to dTG curves in Figures 5, 8 and 9, the

277 ANH and FGDG in the CSAC/calcium sulfate systems did not appear to be fully depleted from day

278 1 so as to give full amounts of ettringite and provide high strengths - possibly due to low reactivity

279 of the calcium sulfate materials. Complete ettringite formation for most of the systems did not

280 seem to occur at least until the 7th day and this may have caused the systems to exhibit lower 1-

281 day strengths than CSAC.

282

283   The use of both FGDG and ANH in CSAC at a proportion of 35% or 50% by mass of the

284   combination gave 28-day strength values meeting the target 42,5 N/R class (Figure 3) and no

285   strength loss was observed up to 90 days. Based on these results and by considering the chemical

286   and dimensional criteria discussed on section 1.1, the selected CSAC/calcium sulfate combinations

287   were those containing 35% FGDG or ANH. The particular content was sufficient to ensure

288   complete ettringite formation and avoid monosulfoaluminate formation as in stoicheiometric

289   calculations. In addition, the content was such that did not appear to cause dimensional instability

290   according to Figure 3.

291

292

293   Compressive strength development of GAF combinations showed that within a maintained

294   CSAC/ANH ratio, the increase of FA at a 15% content gave an increase in 28-day strengths of

295   approximately 3-6 MPa compared to GAF5 and GAF10. Therefore the chosen GAF formulation

296   was the one consisting of 15% by mass of FA, 55% CSAC and 30% ANH as it met the target

297   strength class at maximum percentage of the addition.

298

299

300   *3.3. Hydration*

301
302
303   The hydration processes of CSAC/FGDG, CSAC/PL, CSAC/ANH and GAF15 mixes were

304   investigated through TG, XRD and SEM analyses and each system is discussed below.

305

306

307 *3.3.1 65%CSAC/35%FGDG*

308
309
310 X-ray diffractograms and dTG curves of the stable CSAC/FGDG system are shown in Figures 4

311 and 5 respectively. SEM images of 28-day sample are shown in Figures 6a and b. Based on the

312 diffractograms, the main hydration product was ettringite, and unreacted ye'elimite, gypsum, and

313 gehlenite peaks were also detected. Ettringite corresponding XRD peaks and dTG curves occurred

314 from the first 24 hours of hydration. SEM images showed a homogeneous microstructure with rich

315 amounts of needles within a pore. The prismatic needles had a thickness of approximately 0.5 -2

316 μm and a length ranging from 60 - 100 μm.

317

318

319 Based on the TG analysis, the corresponding weight loss at 115- 135°C and the mass loss was

320 progressively increasing towards the 7th day. At slightly higher temperatures (150-157°C), an

321 additional mass loss was observed, which was assigned to the amounts of gypsum formed in the

322 combination [14]. At 28 days, however, overlapping occurred between corresponding

323 decomposition temperatures of ettringite and gypsum.

324 In temperatures between 265°C - 272°C, alumina hydrates were detected by TG analysis with a

325 mass loss progressively increasing with time (4.25 - 5.46%). This phase was not detectable by

326 XRD analysis due to its non-crystalline structure.

327

328

329 *3.3.2 65%CSAC/35%PL*

330
331
332 X-ray diffractograms and dTG images of CSAC/PL are shown in Figures 7 and 8 respectively.

333 Hydration products were found to be identical to those of CSAC/FGDG at all ages of examination,

334 namely ettringite, gypsum, unreacted ye'elimite and gehlenite. On the first day of hydration,

335 gypsum amounts were excess and a dTG mass loss of this peak reaching almost 6% was observed.

336 Onwards the 28th of hydration, the gypsum amounts were reduced and only a broad peak between

337 gypsum and ettringite was detected. This occurred due to overlapping between the two phases,

338 showing a combined mass loss of the two products. Consequently, the mass loss recorded could

339 not be quantitatively ascribed to ettringite mass loss. The $Al(OH)_3$ had an increasing dTG mass

340 loss reaching up to almost 6.6%, which was comparable to the pattern observed in

341 65%CSAC/35%FGDG.

342
343
344 *3.3.3. 65%CSAC/35%ANH*

345
346
347 Hydration of CSAC/ANH as determined through TG, SEM and XRD is shown in Figures 9, 10a -b

348 and 11 respectively. XRD results showed that the crystalline products of 65%CSAC/35%ANH

349 were equivalent to those of the other two calcium sulfate-based systems, i.e. ettringite, unreacted

350 ye'elimite and gehlenite. Ettringite peaks as shown in Figure 11 became progressively stronger as

351 with the other systems, reaching a maximum on the 28th day of hydration. In this system, no

352 overlapping occurred between dTG gypsum peaks and ettringite peaks, as calcium sulfate was

353 provided solely in the form of anhydrite. Consequently, no hemihydrate dTG peaks were available

354 and therefore quantitative dTG mass losses were entirely ascribed to the amount of ettringite.

355 Towards the 28th day, ettringite mass loss was increasing from approximately 13% to

356 approximately 21.5%. An increase in mass loss of $Al(OH)_3$ was observed (almost 1% increase) on

357 the 28th day compared to day 1.

358

359

360 SEM images (Figure 10a-b) showed rich amounts of prismatic ettringite needles within a pore, and

361 no significant difference in morphology and mineralogy was observed compared to

362 65%CSAC/35%FGDG images.

363

364

365

366 *3.3.4. GAF15 (55%CSAC/30%ANH/15%FA)*

367

368 dTG curves at 1, 3, 7 and 28 days and SEM images at 28 days for GAF15 are shown in Figures 12

369 and 13a -b respectively. X-ray diffractograms at 1, 3, 7 and 28 days of hydration are shown in

370 Figure 14.

371

372

373 According to the results, ettringite was formed from the first day of hydration, with a 4.2% increase

374 in mass loss when reached the 28th day. In particular, the patterns obtained in dTG analysis were

375 similar as in 65%CSAC/35%ANH combination. Crystalline products detected from XRD were

376 ettringite, unreacted ye'elimite, anhydrite and some additional peaks were attributed to the presence

377 of quartz and mullite from the addition of FA and stratlingite appearing onwards the 28th day. The

378 formation of small amounts stratlingite may probably be a result of a reaction between hydrated

379 belite and aluminate-based phases. The XRD peaks of anhydrite were less intense compared to the

380 other systems as the anhydrite was added in lesser amounts in the system (15% calcium sulfate

381 instead of 35% as in the other combinations). $Al(OH)_3$ amounts were comparable to the other

382 combinations, having a dTG mass loss in the range of 5 - 6.6% throughout the period of

383 examination.

384 SEM images of GAF15 in Figures 14a and b showed a dense, homogeneous microstructure

385 consisting of rich amounts of prismatic ettringite needles with unreacted FA particles. The

386 microstructure observed showed a synergistic effect between FA and ettringite. The observed FA

387 particles were immobilized and appeared to be firmly wedged into spaces in-between the formed

388 sulfoaluminate phases, denoting that an effective void filling had occurred.

389

390

391

392   By comparing XRD patterns of CSAC/FGDG, CSAC/PL, CSAC/ANH and GAF15 it can be seen

393   that common hydration products detected were ettringite and unreacted ye'elimite although

394    $Al(OH)_3$ could not be detected due to its non-crystalline structure. Gypsum was detected at

395   CSAC/FGDF and CSAC/PL, whereas anhydrite was detected in GAF15 and CSAC/ANH.

396   Ettringite XRD peaks were more intense in CSAC/ANH and GAF15 than in CSAC/PL and

397   CSAC/FGDG, particularly at an angle of 26.5^{o}, probably due to the overlapping peak of anhydrite.

398   In the GAF15, quartz and mullite were additionally detected due to the FA incorporated in the

399   combination.

400

401   *3.4. Isothermal conduction calorimetry*

402

403

404   Heat patterns and accumulated output rates of CSAC/ANH, GAF15 and CSAC/FGDG systems are

405   shown in Figure 15. Measurements of heat of hydration for the CSAC/PL could not be obtained as

406   the combination suffered from rapid setting and no time was given for preparation of the sample.

407

408

409   GAF15 heat pattern showed an initial shoulder peak occurring in less than 2 hours, followed by a

410   maximum heat rate between the 5th and the 6th hour. Peaks were associated with the depletion of

411   calcium sulfate and the formation of sulfoaluminate and aluminate hydrates. Output peak rates

412   were higher in GAF15 combination. CSAC/ANH showed a heat pattern similar to that of GAF15

413   but with lower maxima and equivalent peaks delayed at approximately 2 hours compared GAF15.

414   Both the combinations showed the same tendency of exhibiting an initial shoulder followed by a

415   heat peak maximum. In CSAC/FGDG, only one main peak was detected 2 and 4 hours earlier than

416   those of GAF15 and CSAC/ANH respectively. This reflected the tendency of hemihydrate to

417   accelerate the formation of both sulfate hydrate and sulfoaluminate hydrate phases simultaneously.

418   The particular peak was attributed to the formation of gypsum and ettringite, both having occurred

419   at the same period. A smooth curve was also observed after a period of dormancy, having a

420   maximum heat output rate of less than 2 W/kg at 17 hours, probably due to the precipitation of

421   further sulfoaluminate and aluminate-based phases.

422

423   *3.5 Initial and final setting times*

424
425
426   Comparison of the initial and final setting times between all examined cements is shown in Figure

427   16.

428

429

430   Generally, the initial setting of almost all cements/combinations occurred at the beginning of their

431   accelerating heat pattern period and final setting times occurred before the corresponding heat

432   output maxima. In all CSAC/calcium sulfate combinations regardless of the presence of FA,

433   setting times were shorter than those of a typical Portland cement-based combination, mainly

434   because of the high water demand during ettringite formation. It is known that 32 molecules of

435   water are attracted on the ettringite skeletal structure according to the phase chemical composition.

436   In contrast, the C-S-H is associated with fewer molecules regardless of its stoicheiometric

437   variations. Main factors influencing the water adsorption rate in ettringite are mainly the

438   morphology, the crystalline structure, the phase size (larger than C-S-H) and the interlocking effect

439   between the compounds. Comparing the behaviour of CSAC/FGDG to that of typical CEM I

440   systems, the results suggest that setting times would not normally raise concerns in construction

441   processes when considering transportation and casting. By comparing, however the setting

442   behaviours of the CSAC/FGDG and CSAC/PL systems (i.e. two CSAC/hemihydrate systems), it

443   can be seen that there is a notable difference in initial and final sets. This may be attributed to the

444   reactivity and solubility of the two materials which might have been affected by the presence of

445   moisture from the production process and/or any impurities present [14].

446

447

448   The incorporation of FA in the CSAC/ANH combination (i.e. the GAF15) caused a reduction on

449   the final setting time -approximately 40 minutes- whilst no effect on initial setting times occurred.

450   The explanation for these results lies on the calorimetric curves and the cumulative heats of the two

451   combinations (Figures 15). It can be seen that the initial shoulder peak in GAF15 was higher and

452   occurred faster than that of CSAC/ANH. This reflected an earlier consumption of calcium sulfate

453   and formation of the hydrates. Consequently a higher water demand caused final sets to reduce in

454   GAF15. Moreover, cumulative heats of GAF15 were still higher than those of CSAC/ANH,

455   regardless of the fact that ettringite amounts were lesser in GAF15 (a TG mass loss approximately

456   2.5% lower than that of CSAC/ANH), due to the reduced CSAC and anhydrite contents in the

457   combination,

458

459   The incorporation of PL in CSAC had the most considerable effect on setting times. Values were

460   unacceptably short and during the mixing process, rapid setting occurred without allowing any

461   margin for sample preparation, compaction and finishing. The final setting time was taken as less

462   than 5 minutes. As evidenced, most of the techniques adopted for investigation of the cements

463   could not be conducted for this particular combination. This may likely reflect the particular

464   hemihydrate's impractical use and it may probably raise concerns when considering applications.

465   Such behaviour would most probably be associated with the substantially high reactivity of

466   calcium sulfate hemihydrate, therefore plaster-based CSAC combinations may not constitute the

467   most appropriate solution for use in construction unless admixtures that retard the setting times and

468   prolong the fresh semi-plastic state of the paste are introduced.

469

470   CSAC/FGDG setting times were higher than those of CSAC/ANH and GAF15 probably due to the

471   variability of the commercial product, in combination with the presence of impurities that

472   ultimately affected its reactivity.

473

4. Conclusions

Given the need for the utilization of alternative cementitious systems to reduce the environmental impact associated with Portland cement manufacture, alternative cementitious systems of lower eCO_2, when optimally proportioned and based on calcium sulfoaluminate- calcium sulfate-fly ash, may potentially offer environmental benefits. The following conclusions are made according to the results of this paper:

- The use of FA in CSAC in the presence of anhydrite promoted an earlier formation of a strong ettringite-rich matrix, firmly accommodating FA particles with earlier final sets. Both the FA particles and the formed hydrated phases appeared to synergistically contribute to a dense microstructure. Accumulated heat outputs and early strengths reached higher values than those of the pure CSAC/ANH and CSAC/FGDG combinations.

- The use of hemihydrate and anhydrite calcium sulfate in combination with CSAC had a notable effect on the rate of hydration, setting times, and to a lesser extent the mechanical performance of the system. The incorporation of anhydrite in the CSAC appeared to be more mechanically beneficial than that of any hemihydrate form. No significant differences were found in the mineralogy and morphology of the hydration products at different introduced forms of calcium sulfate at 35% by mass. In the hemihydrate-based systems, gypsum formation occurred at very early hydration stages and this was detectable by TG and XRD. $Al(OH)_3$ quantities were comparable at all CSAC/calcium sulfate systems as shown by TG. The use of hemihydrate (FGDG) was found to accelerate the formation of phases, based on the heat patterns.

498   • The incorporation of hemihydrate in CSAC caused unacceptably short setting times of the

499   CSAC/PL combination without allowing a time margin for sample preparation in most techniques.

500   This may render the use of hemihydrate impractical within CSAC/calcium sulfate systems and it

501   may raise concerns when considering applications. Such behaviour is associated with the

502   substantially high reactivity and solubility of hemihydrate compared to that of anhydrite.

503   Therefore, plaster-based CSAC combinations may not be regarded as the most appropriate solution

504   for certain applications unless admixtures that retard the setting times are introduced. The most

505   advantageous form of calcium sulfate for the CSAC system appeared to be the anhydrite form.

506

507

508

509   **Acknowledgements**

510
511

515

516 **References**

517

518 [1] OECD/IEA and The World Business Council for Sustainable Development. "Cement

519 technology Roadmap 2009 – Carbon emissions reductions up to 2050" Switzerland: Atar Roto

520 Rresse SA. Available at: http://www.wbcsd.org/ [Last accessed 24 Jul 12]

521

522

523 [2] G. Hammond and C. Jones, Inventory of Carbon and Energy (ICE) , University of Bath.

524 Available at http://www.bath.ac.uk/mech-eng/sert/embodied/ [Last accessed 24 May 2012]

525

526

527 [3] L. Zhang , M.Z.Su, Y.M. Wang, Development of the use of sulfo- and ferro-aluminate cements

528 in China, Adv. Cem. Res, 11 (1999) 15– 21.

529

530

531 [4] P. Arjunan , M.R. Silsbee, D.M. Roy, Sulfoaluminate-belite cement from low calcium fly ash

532 and sulfur rich and other industrial by-products, Cem. Concr. Res. 29 (8) (1999) 1305–1311.

533

534

535 [5] C.D, Lawrence. The production of low-energy cements, in: J. Bensted, P. Barnes, eds.

536 Structures and performance of cements. Spon Spress, London, 2002.

537

538

539 [6] I. Janotka and L.Krajci , An experimental study on the upgrade of sulfoaluminate belite cement

540 systems by blending with Portland cement, Adv. Cem. Res. 11 (1999) , 35-41.

541

542

543   [7] E. Gartner, Are there any practical alternatives to the manufacture of Portland cement clinker?

544   Proceedings of the 11th International Conference on Non-conventional Materials and Technologies

545   NOCMAT, 6-9 September 2009, Bath: University of Bath.

546

547

548   [8] F. Glasser , L.Zhang "High-performance cement matrices based on calcium sulfoaluminate–

549   belite compositions". Cem. Concr. Res 31 (12) (2001), 1881-1886.

550

551

552   [9] J. Pera , J. Ambroise , New applications of calcium sulfoaluminate cement, Cem. Concr. Res

553   2003; 34 (4) (2003) 671-676.

554

555

556   [10] K. Quillin K, Low energy cements. BR 421, IHS BRE Press, 2001.

557

558

559   [11] S. Ioannou, K.A. Paine , K. Quillin, Strength and durability of calcium sulfoaluminate based

560   concretes, Proceedings of the 12th International Conference on Non-conventional Materials and

561   Technologies NOCMAT, 21-23 September 2010, Cairo: HBRC.

562

563

564   [12] E. Gartner, Industrially interesting approaches to ''low-CO_2" cements. Cem. Concr. Res 34

565   (9) (2004) 1489–1498.

566

567

568   [13] M.C.G. Juenger, F. Winnefield, J.L Provies, J.H. Ideker, Advances in alternative cementitious

569   binders. Cem.Concr.Res. 41 (12) (2010) 1232-1243.

570

571

572   [14] M.V. Borrachero, J. Payá, M. Bonilla M., J. Monzó,. The use of thermogravimteric analysis

573   for the characterization of construction materials:The gypsum case, J.therm.anal.calorim. 91 (2)

574   (2008) 503-509.

575

576

577   [15] R.X.Hao, and X.Y Guo, X.Y, The properties of flue gas desulphurization (FGD) gypsum,

578   Appl. Mech. Mater. 05 (2012) 2204-2208.

579

580

581   [16] PowerTech, Instruction Sheet: Analysis of FGD Gypsum. 2nd ed. Essen: VGB PowerTech

582   E.V, 2008

583

584

585   [17] V. Živica, Properties of blended sulfoaluminate belite cement Constr. Build. Mater 14(8)

586   (2000), 433-437.

587

588

589   [18] BS EN 450-1:2012 *Fly ash for concrete - Definition, specifications and conformity criteria.*

590   British Standards Institution.

591

592

593

[19] BS EN 196-3:1995. *Methods of testing cement - Part 3: Determination of setting times and soundness.* British Standards Institution.

596

597

598

599

[20] BS EN 196-1:1995. *Methods of testing cement - Part 1: Determination of strength.* British Standards Institution

602

603

604

[21] BS EN 197-1:2000. *Cement - Part 1: Composition, specifications and conformity criteria for common cements.* British Standards Institution.

607

608

609

[22] F. Winnefeld and Lothenbach, B. Thermodynamic modelling of the hydration of calcium sulfoaluminate cements, Proceedings of the International Summit on the Hydration Kinetics, 27-29 July 2009, Canada: Laval University.

613
614

615 **LIST OF FIGURES**

616

617 *Figure 1. Dimensional changes of CSAC/ANH combinations at varying ANH contents*

618

619

620 *Figure 2. Dimensional changes of CSAC/FGDG combinations at varying FGDG contents*

621

622

623 *Figure 3. 28-day strength of CSAC/FGDG and CSAC/ANH at varying calcium sulfate content and*

624 *limits of stability*

625

626

627 *Figure 4   X-Ray diffractograms of 65%CSAC/35%FGDG   obtained at 1, 3, 7 and 28 days of*

628 *hydration*

629

630

631 *Figure 5 dTG curves and mass losses in 65%CSAC/35%FGDG obtained at 1, 3, 7 and 28 days of*

632 *hydration.*

633

634

635 *Figures 6a and b SEM image of 65%CSAC/35%FGDG obtained at 28 days.*

636

637

638 *Figure 7. X-ray diffractograms of 65%CSAC/35%PL at 1,3,7 and 28 days of hydration*

639

640

641 *Figure 8. dTG curves of 65%CSAC/35%PL at 1,3,7 and 28 days of hydration*

642

643

644 *Figure 9. dTG curves of CSAC/ANH at 1, 3, 7 and 28 days of hydration*

645

646

647   *Figures 10a and b SEM Image of 65%CSAC/35%ANH at 28 days of hydration*

648

649

650   *Figure 11. X-ray diffractograms of 65%CSAC/35%ANH at 1,3,7 and 28 days of hydration*

651

652

653   *Figure 12. dTG curves of GAF15 at 1,3,7 and 28 days of hydration*

654

655

656   *Figure 13a and b SEM image of GAF15 at 28 days of hydration*

657

658

659   *Figure 14. X-ray diffractograms of GAF15 at 1,3,7 and 28 days of hydration*

660

661

662   *Figure 15. Heat patterns and accumulated heat output rates of CSAC/FGDG, CSAC/ANH, and*

663   *GAF15*

664

665

666   *Figure 16. Initial and final setting times of the investigated cements*

667
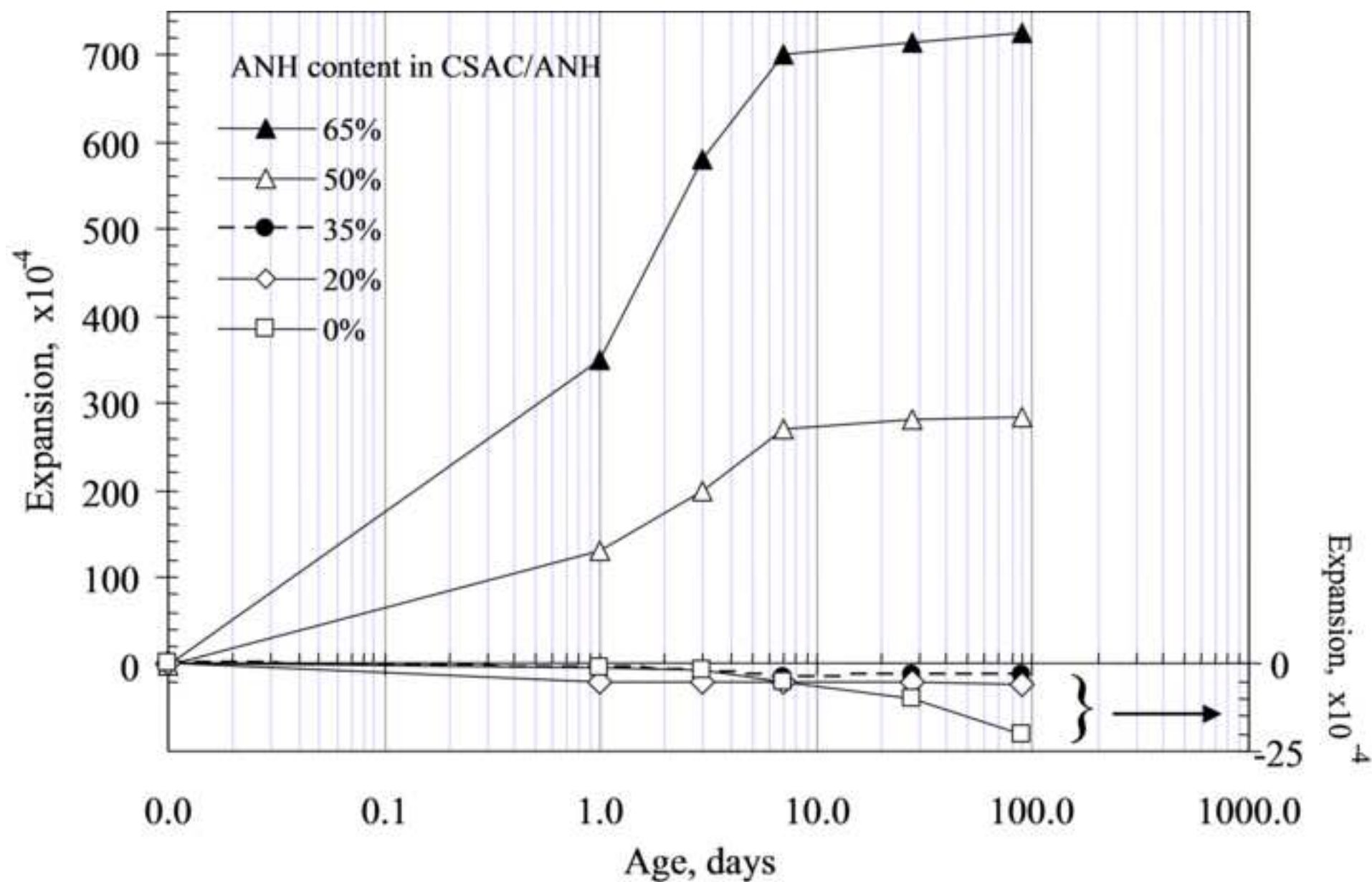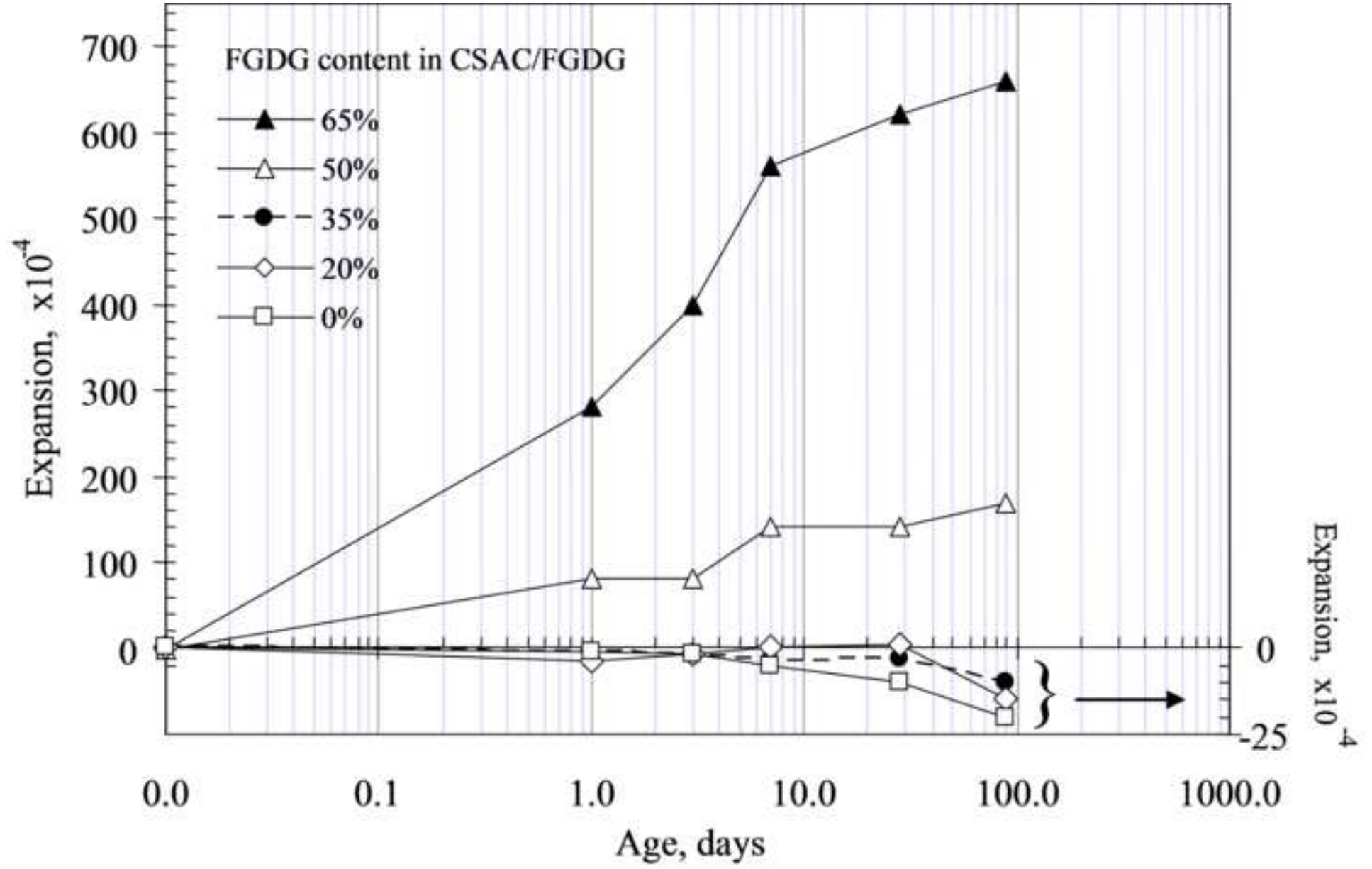
Figure_3
Click here to download high resolution image
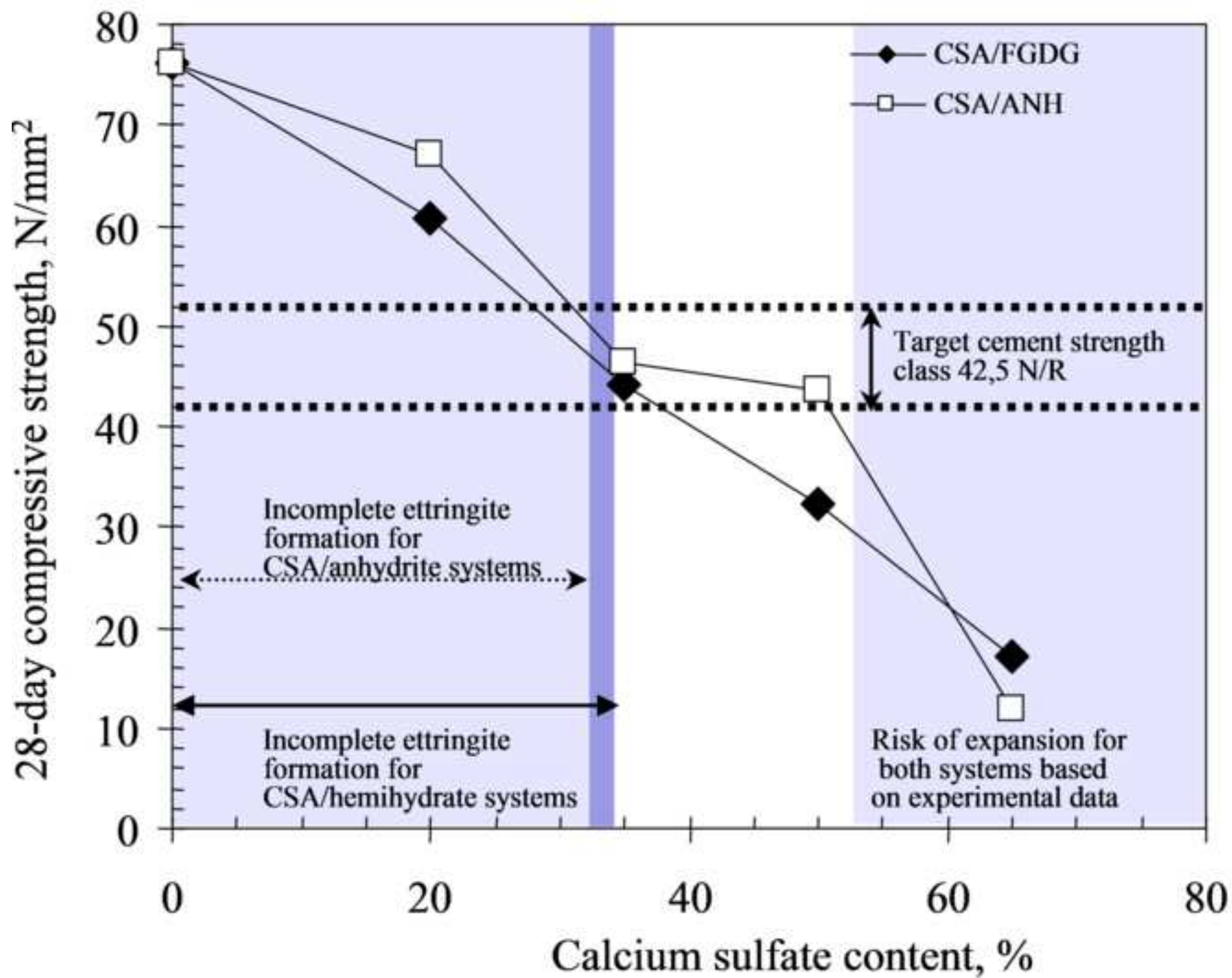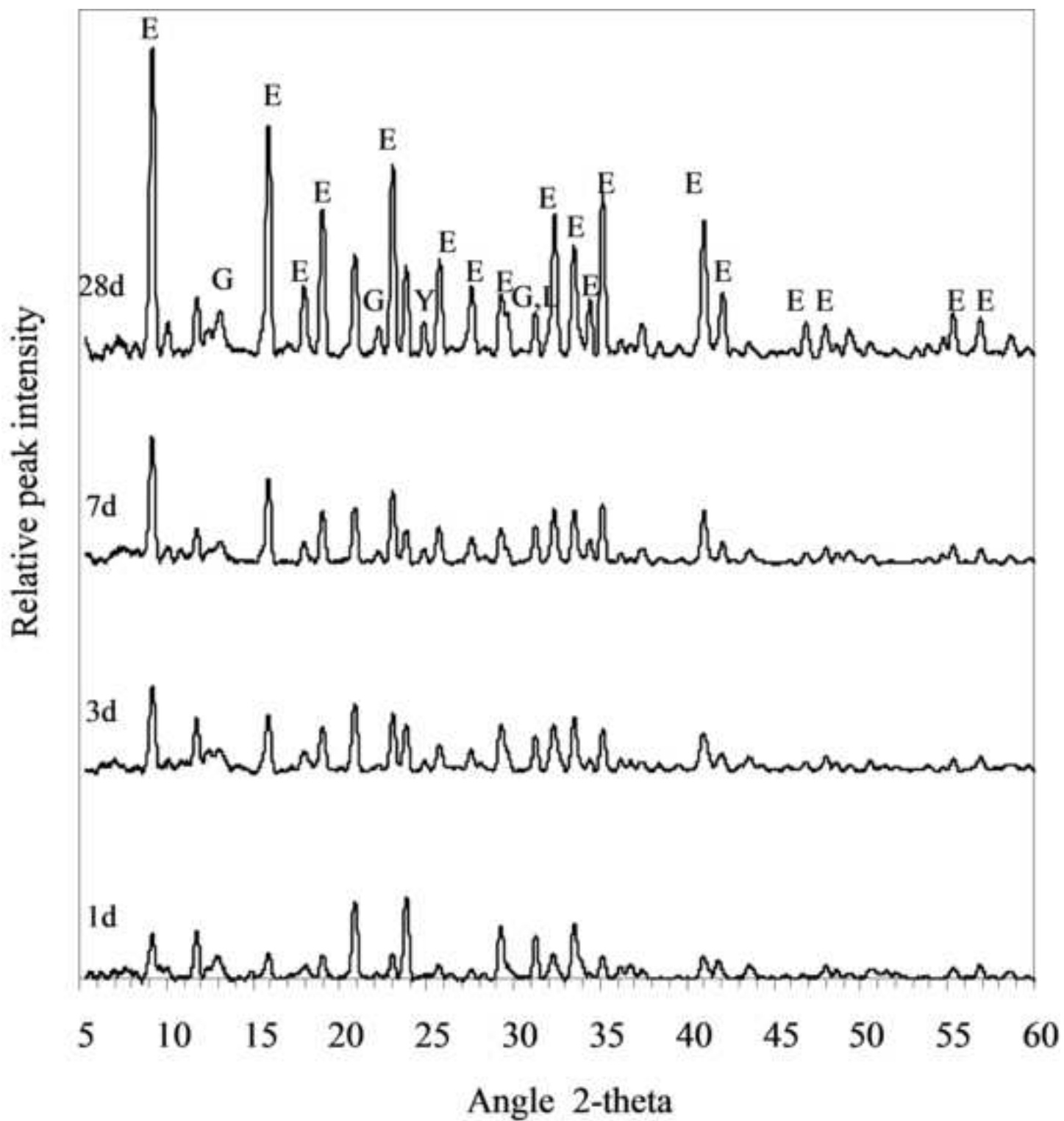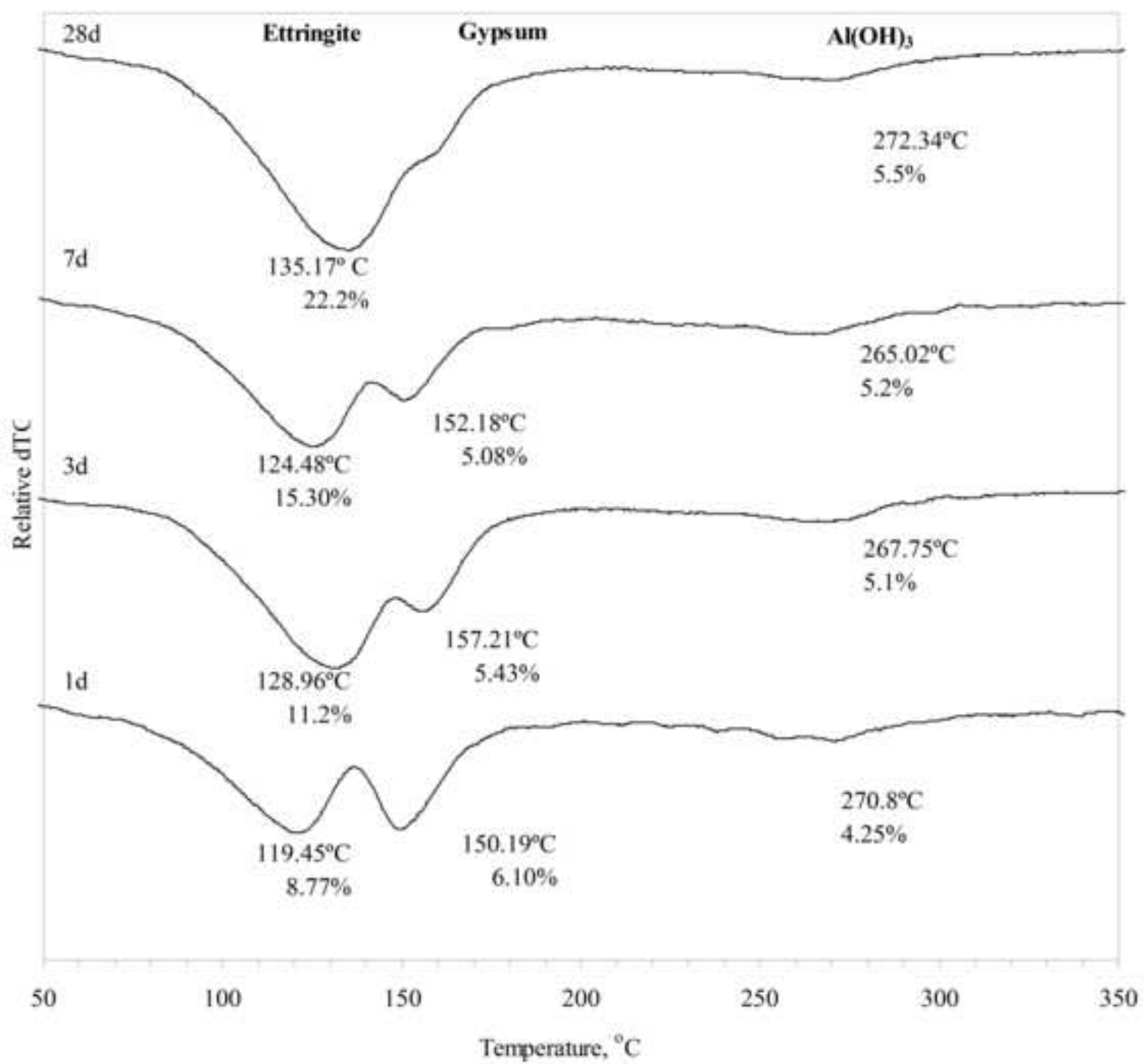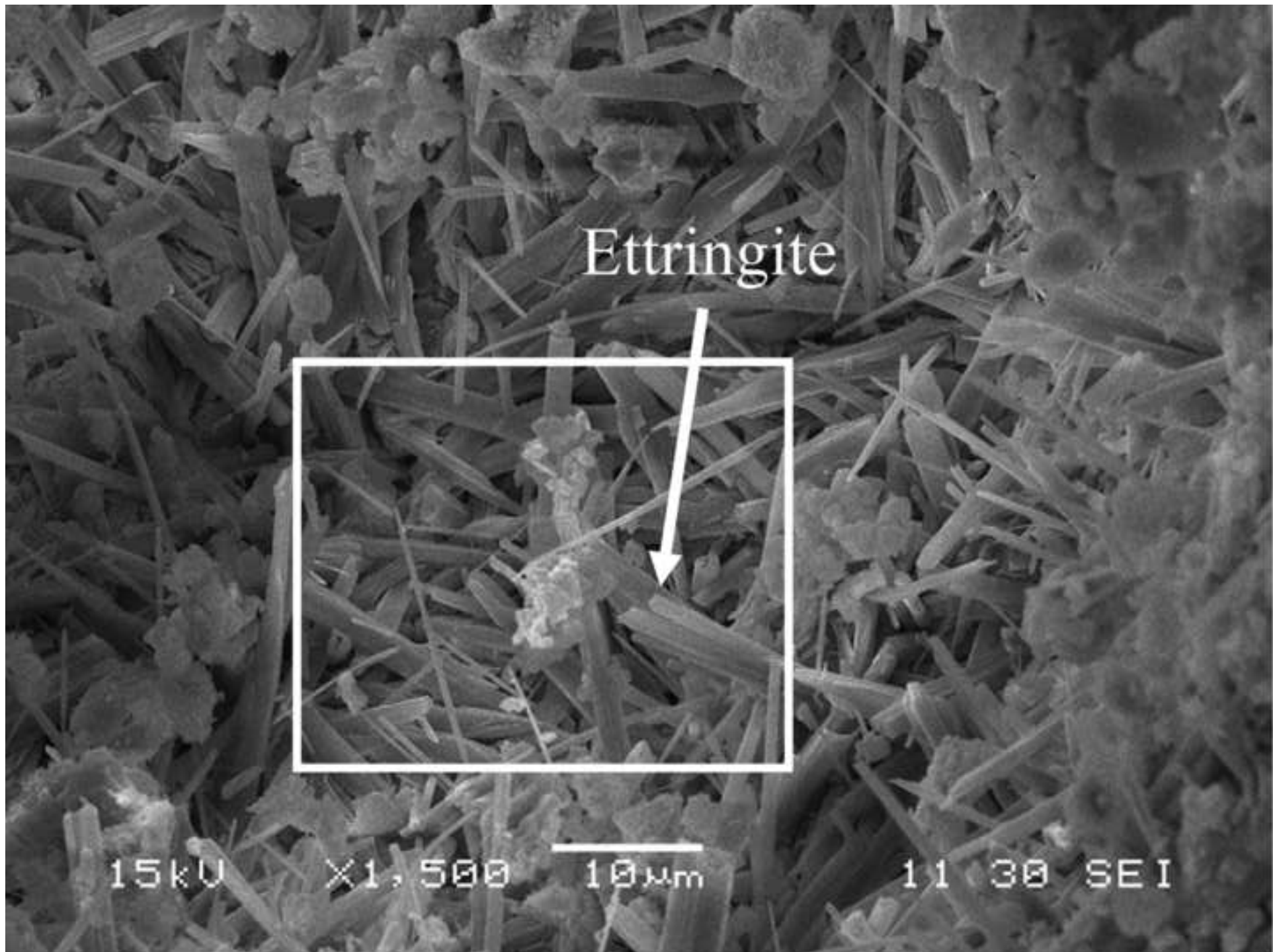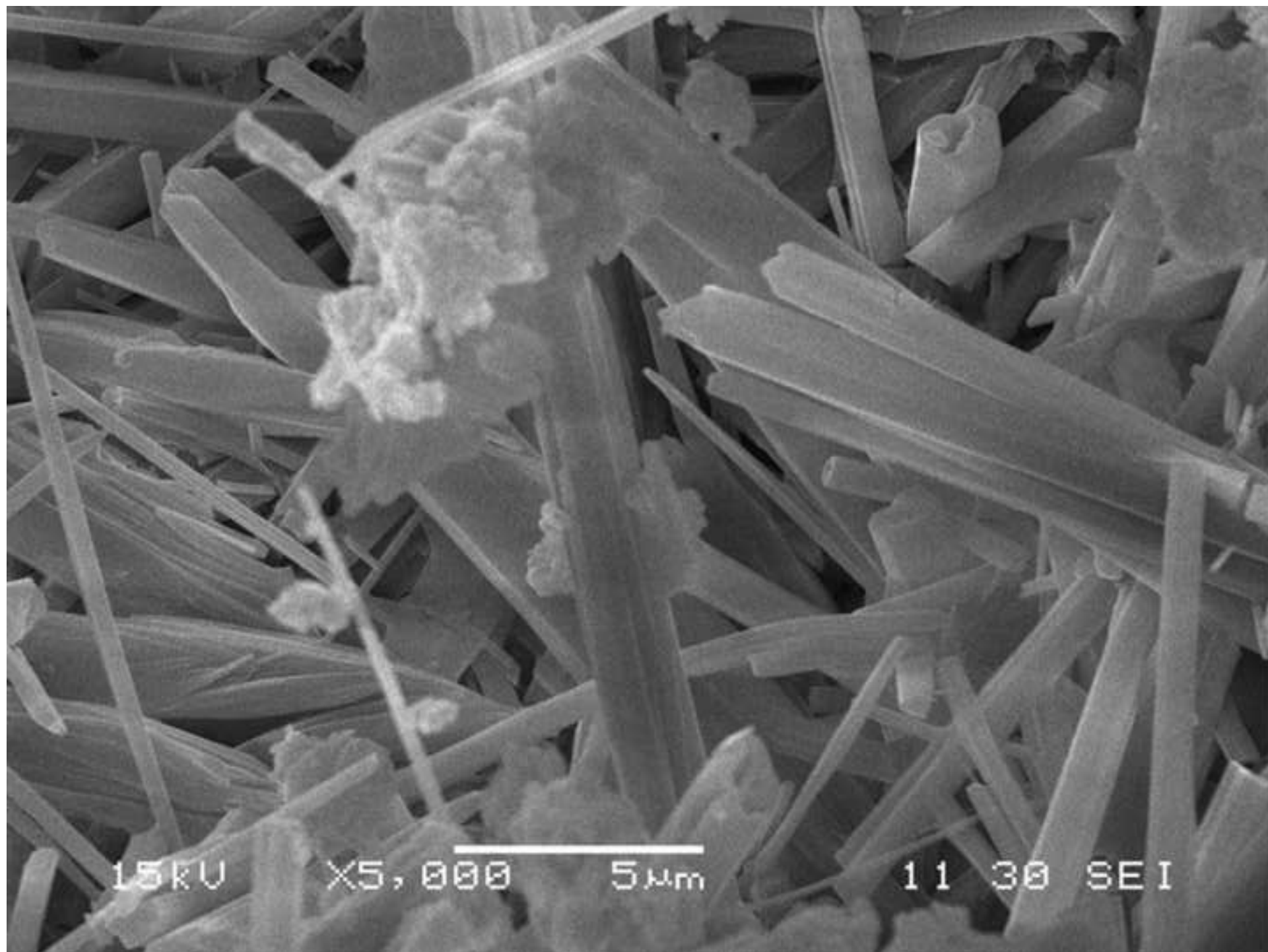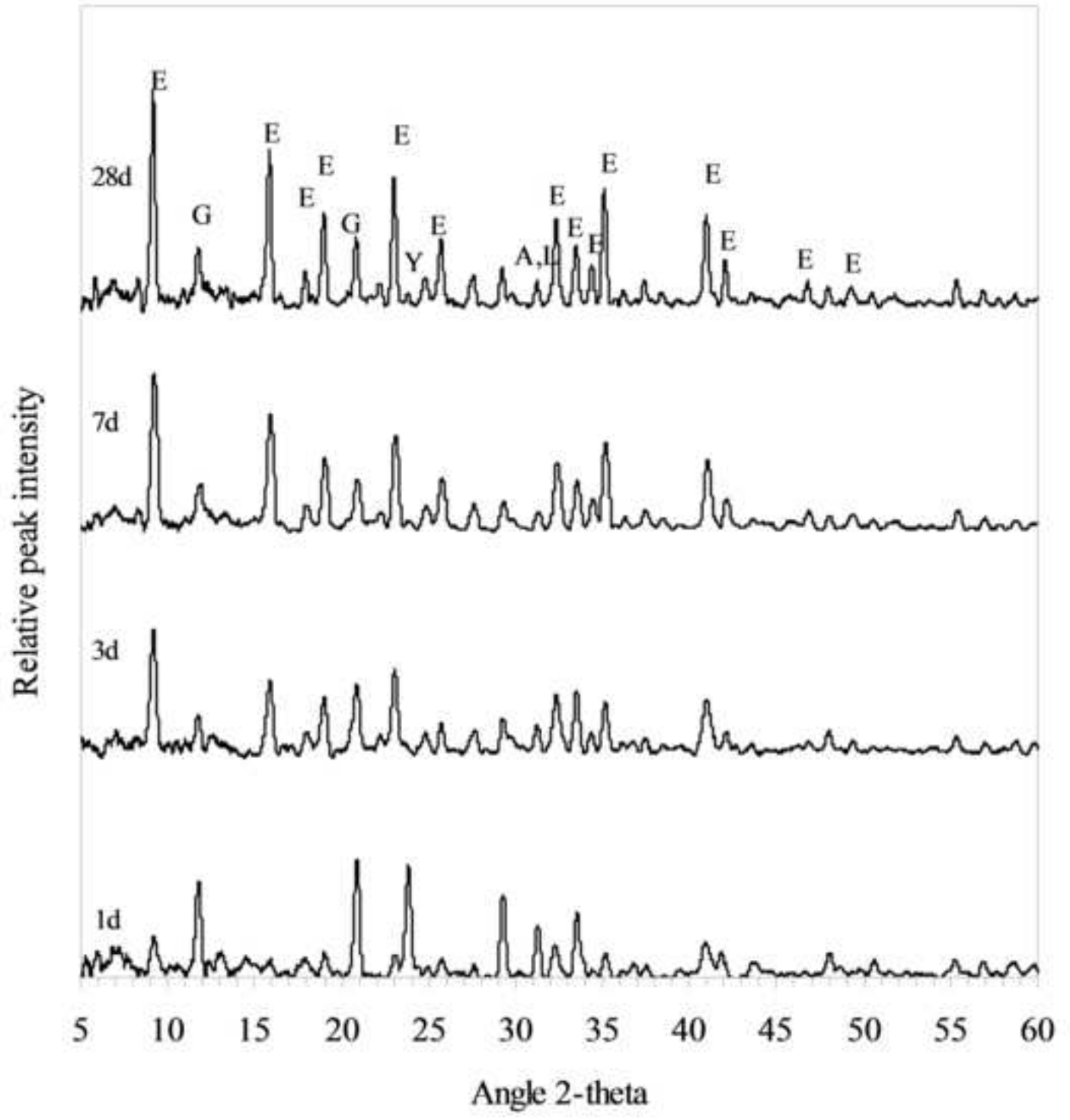
Figure_7

Figure_8
Click here to download high resolution image

Figure showing Relative dTG vs Temperature (°C) curves for samples at 1d, 3d, 7d, and 28d, with peaks labeled Ettringite, Gypsum, and Al(OH)₃.

28d:
140.98°C, 26.28%
276.80°C, 6.59%

7d:
132.80°C, 21.37%
271.33°C, 6.08%

3d:
121.44°C, 11.75%
148.55°C, 3.92%
271.20°C, 6.05%

1d:
114.05°C, 7.91%
147.29°C, 5.95%
267.86°C, 4.46%
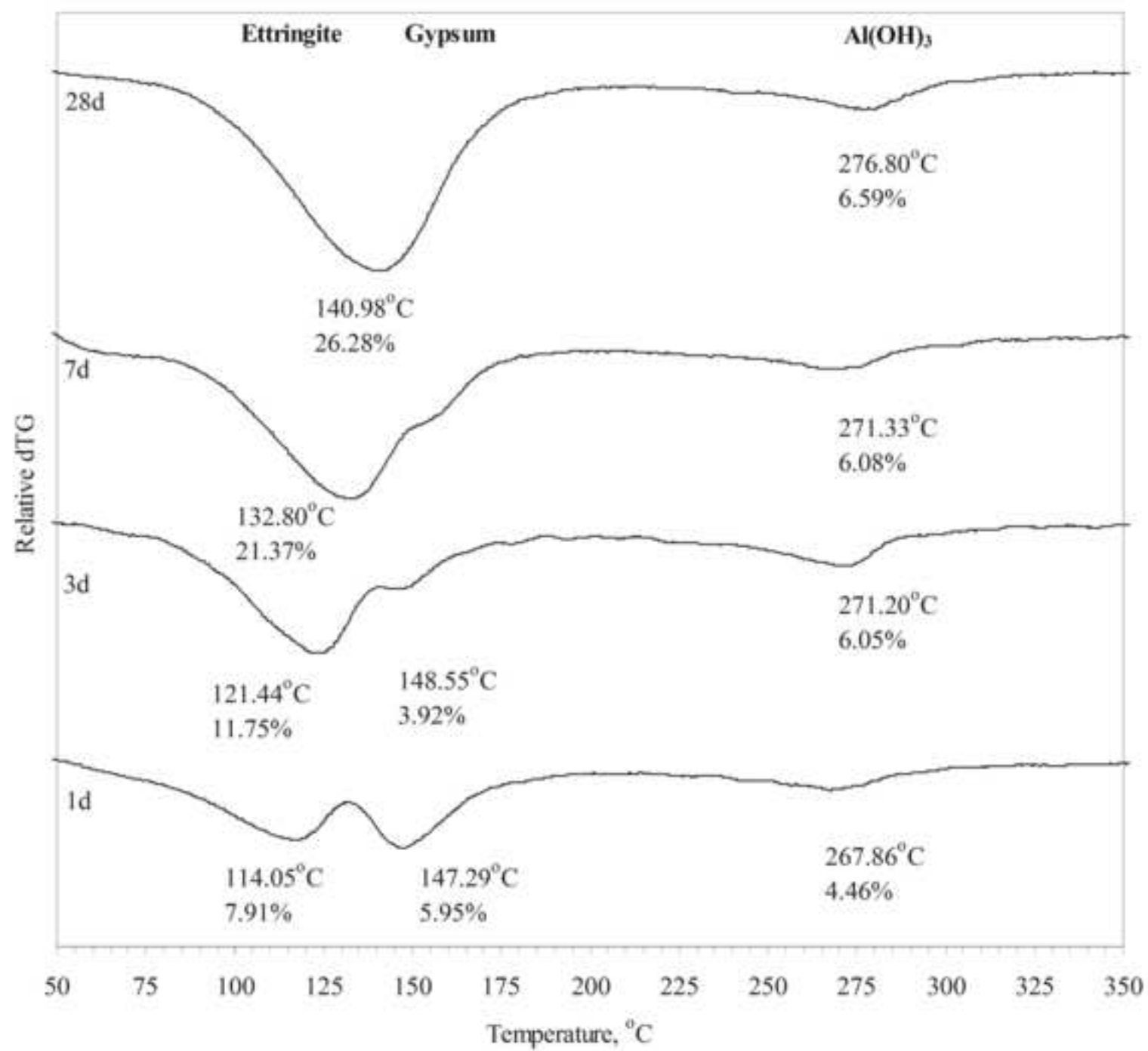
Figure_9
Click here to download high resolution image
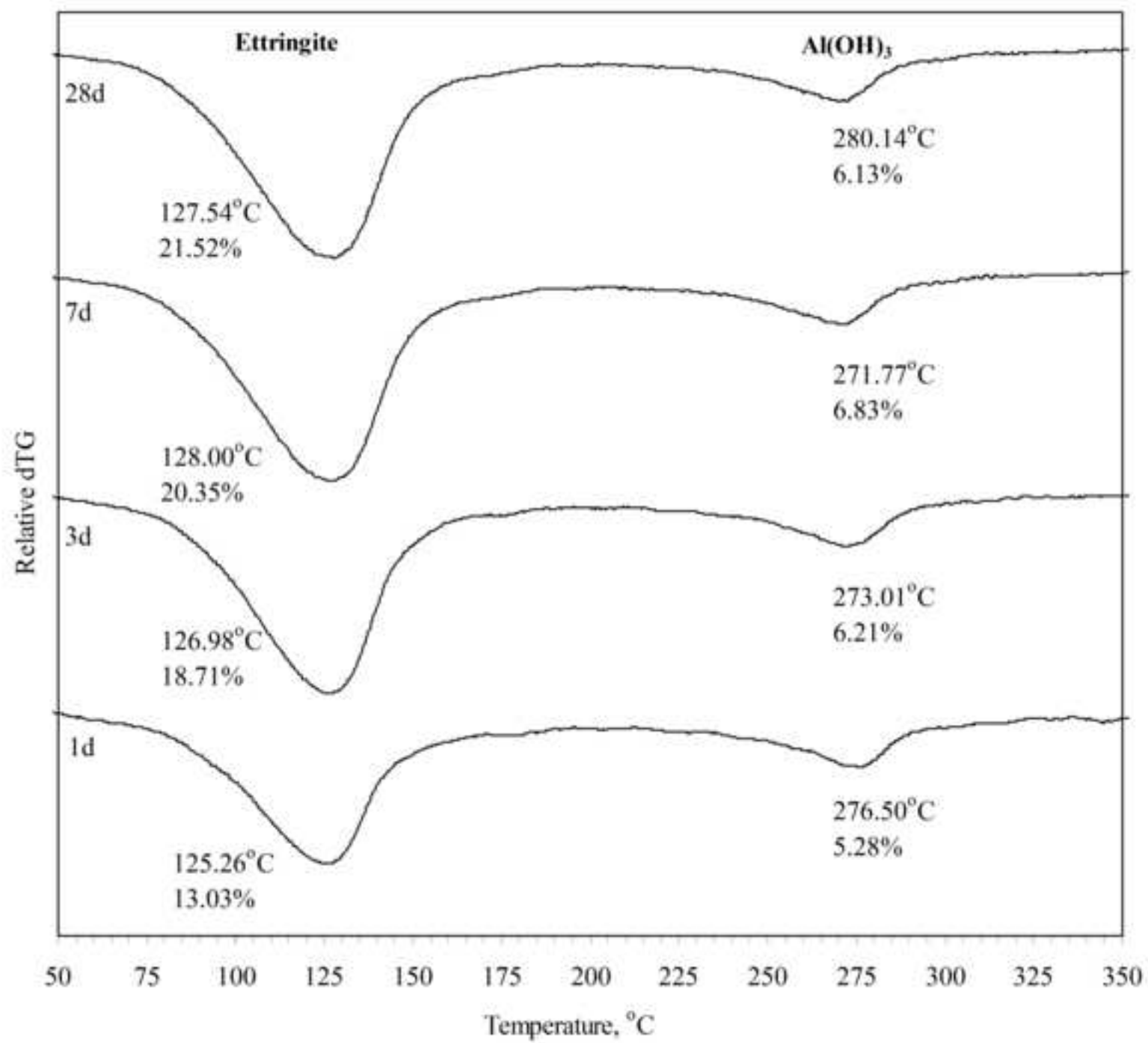
15kV   X1,000   10μm   09 50 SEI
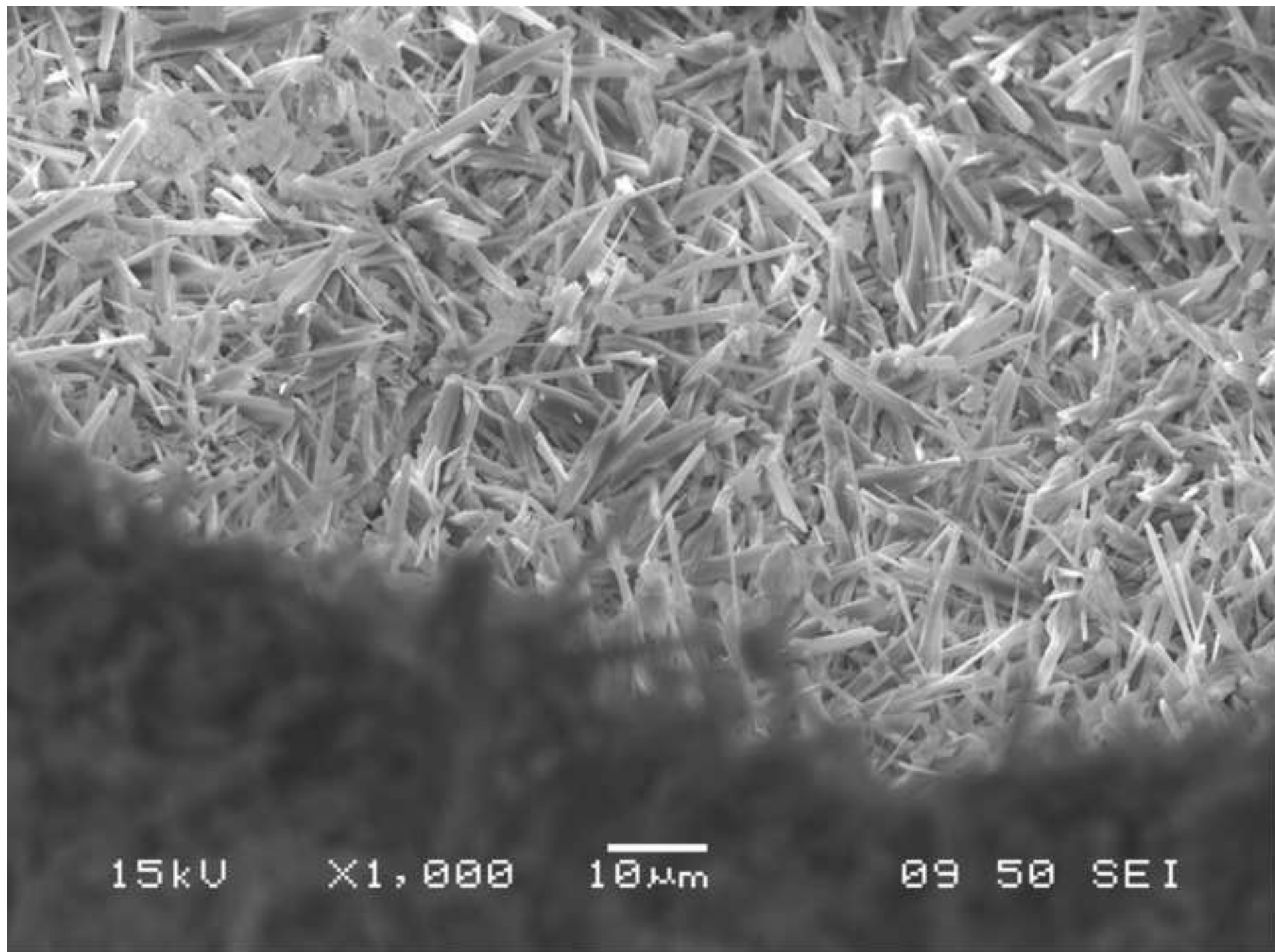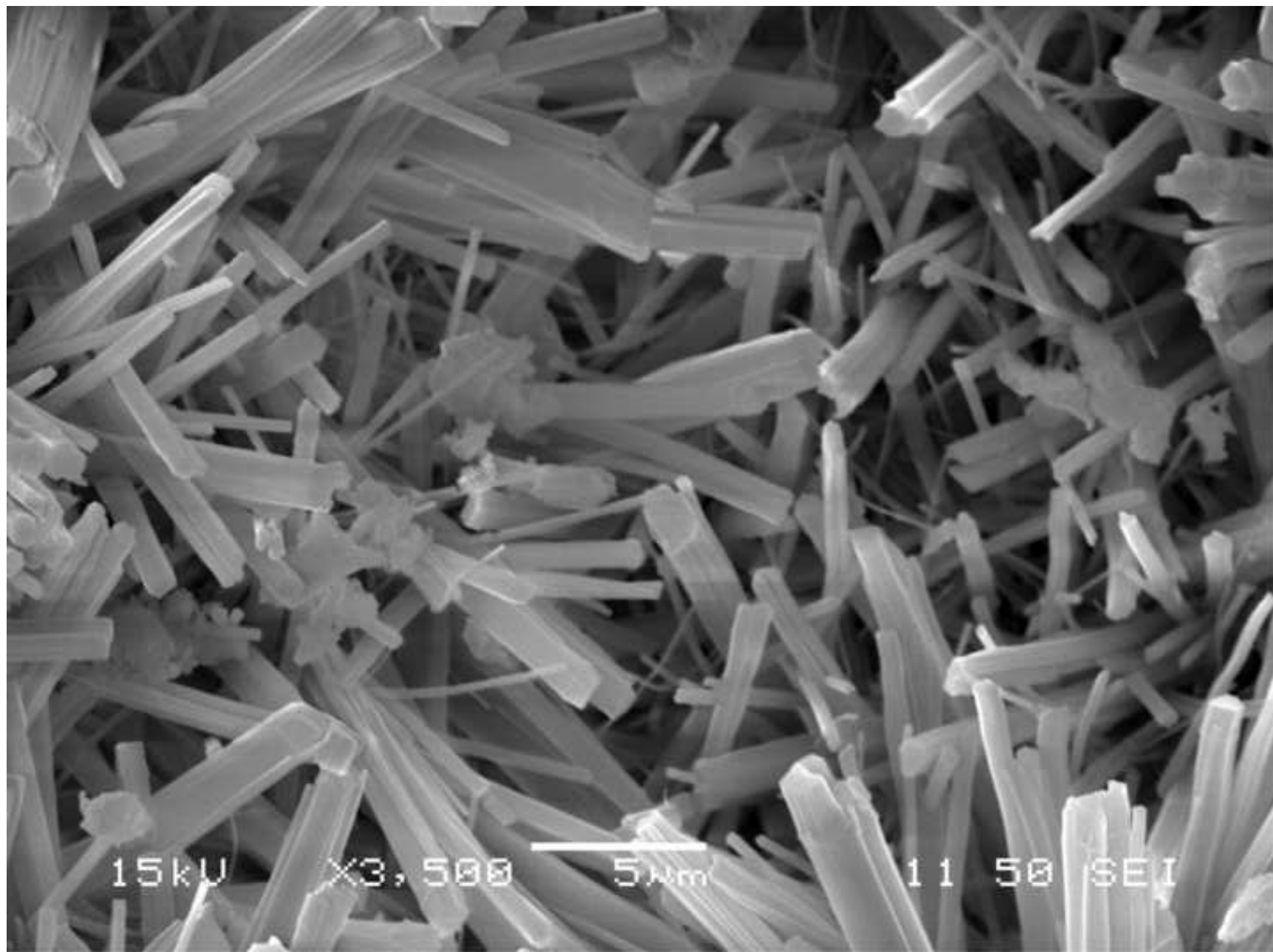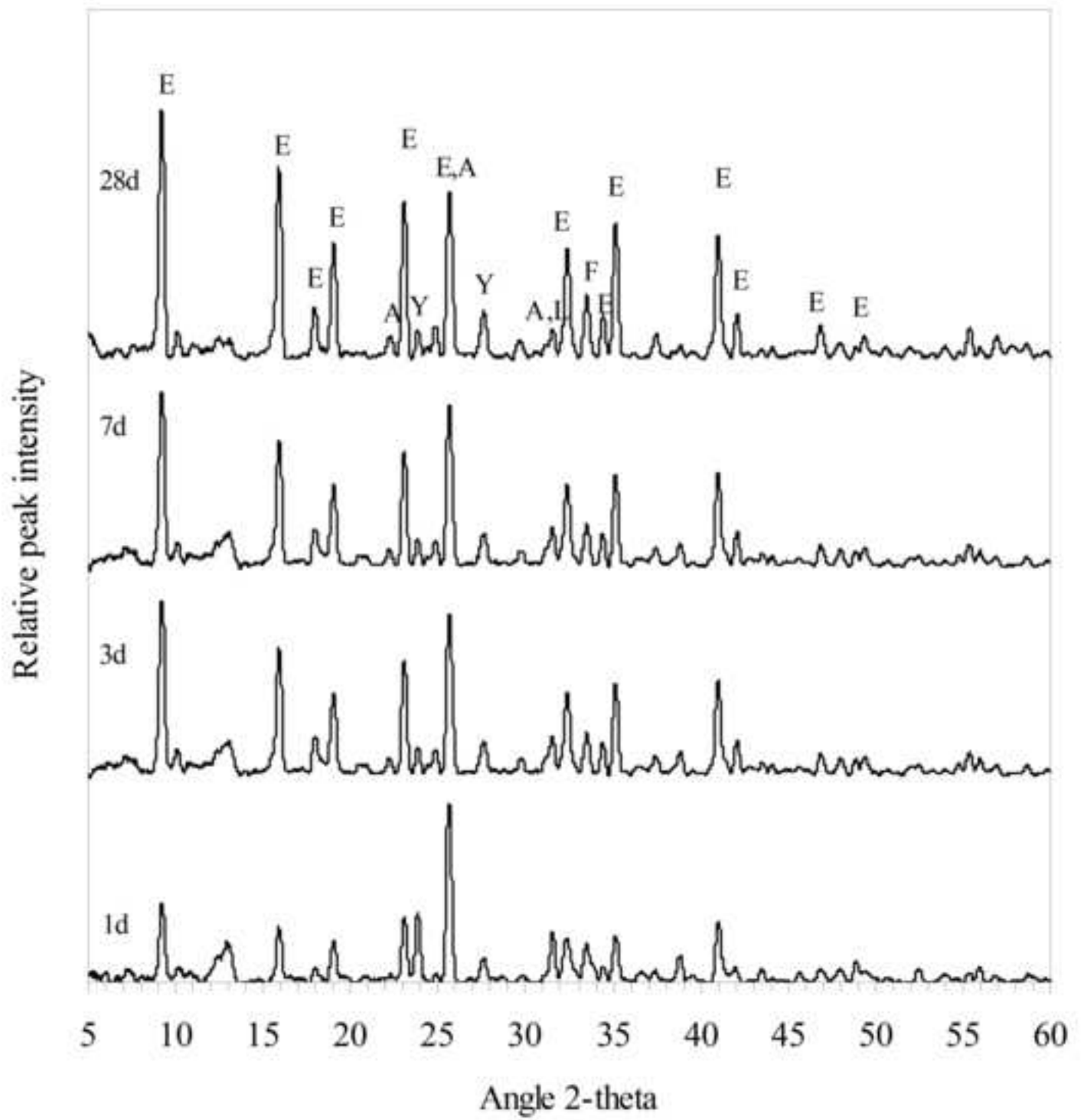
Figure_10b

Figure_12
Click here to download high resolution image
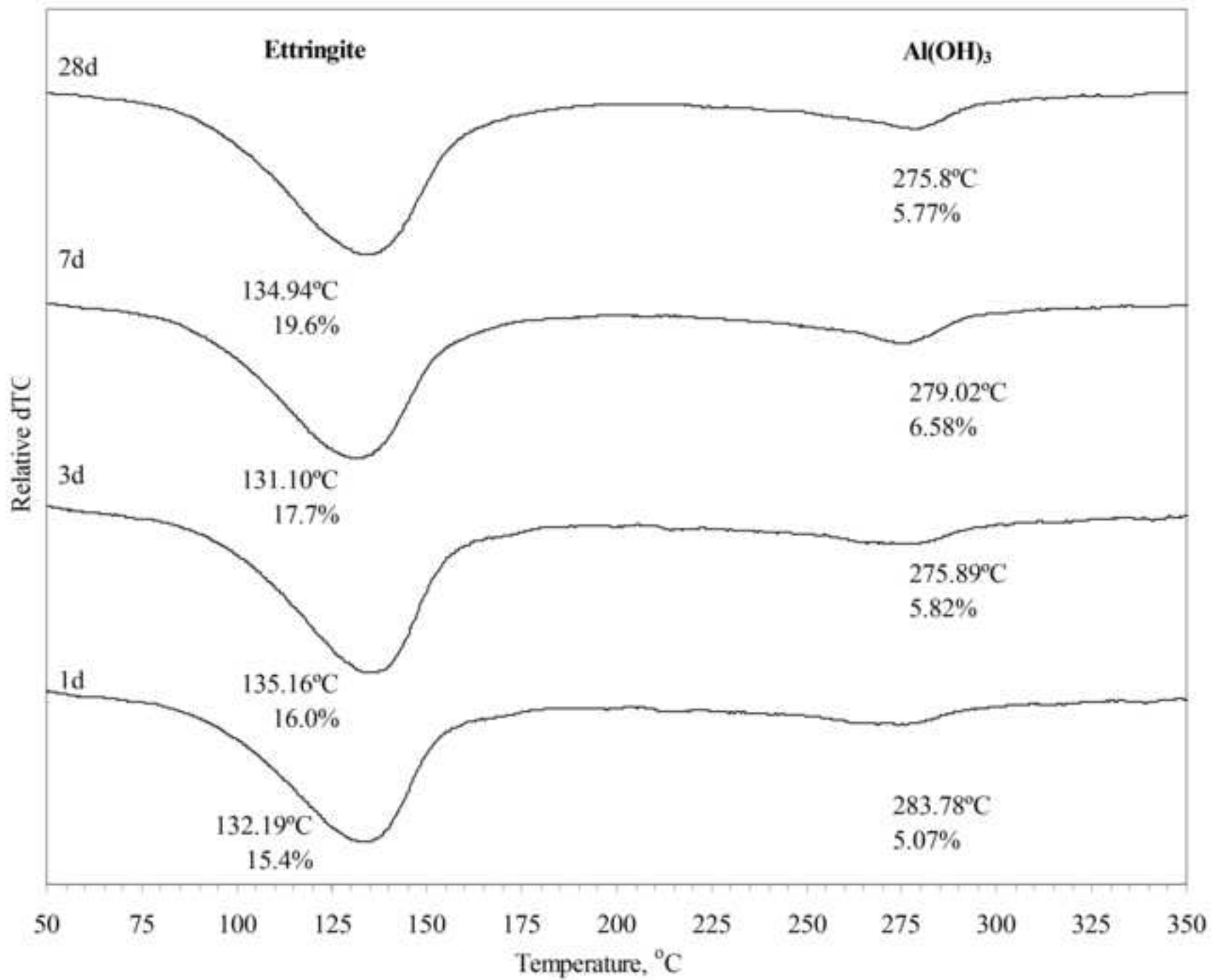
Ettringite   Al(OH)$_3$

28d

275.8°C
5.77%

7d

134.94°C
19.6%

279.02°C
6.58%

3d   131.10°C
17.7%

275.89°C
5.82%

1d   135.16°C
16.0%

283.78°C
5.07%

132.19°C
15.4%

Relative dTC

50   75   100   125   150   175   200   225   250   275   300   325   350

Temperature, °C
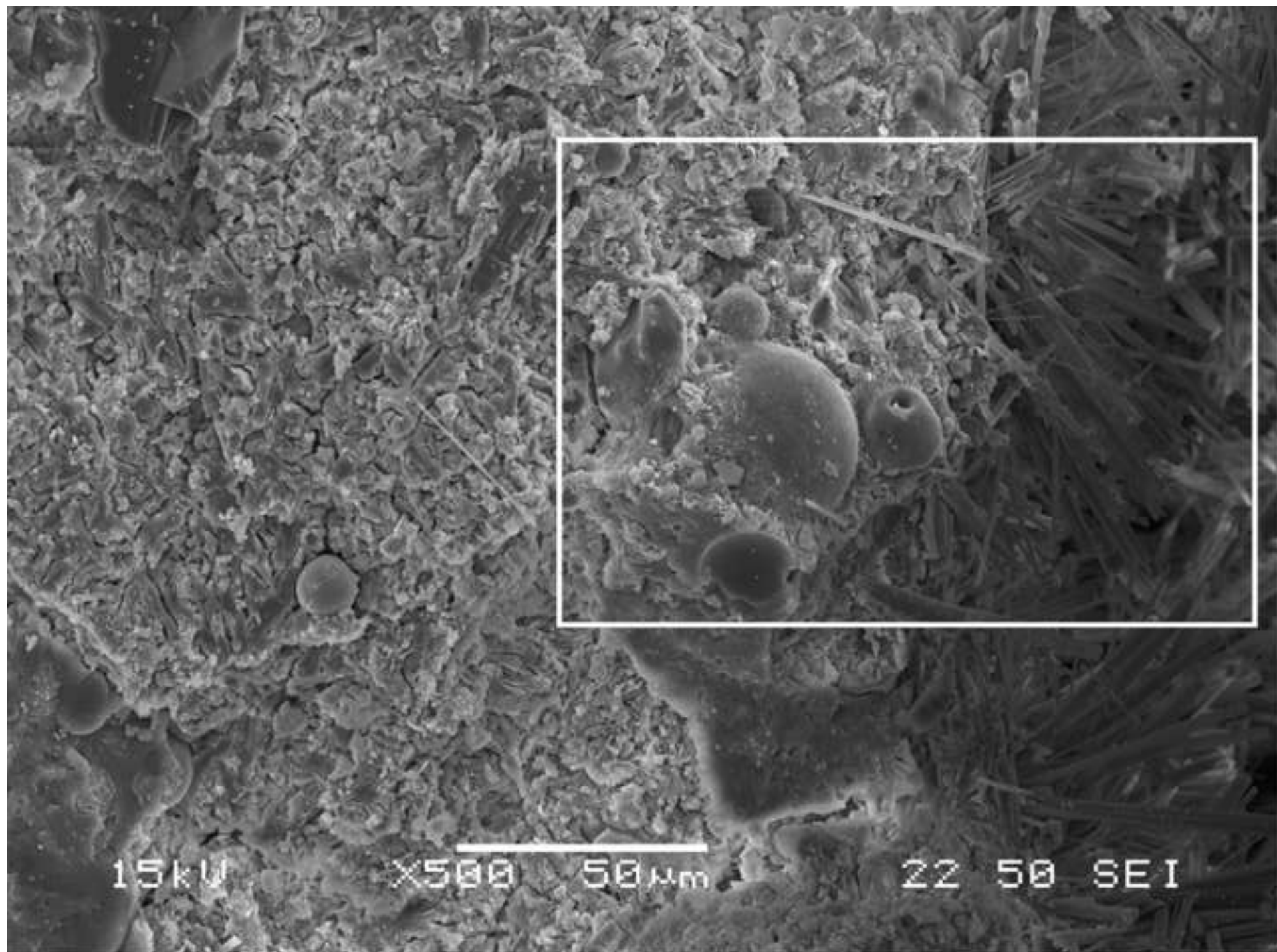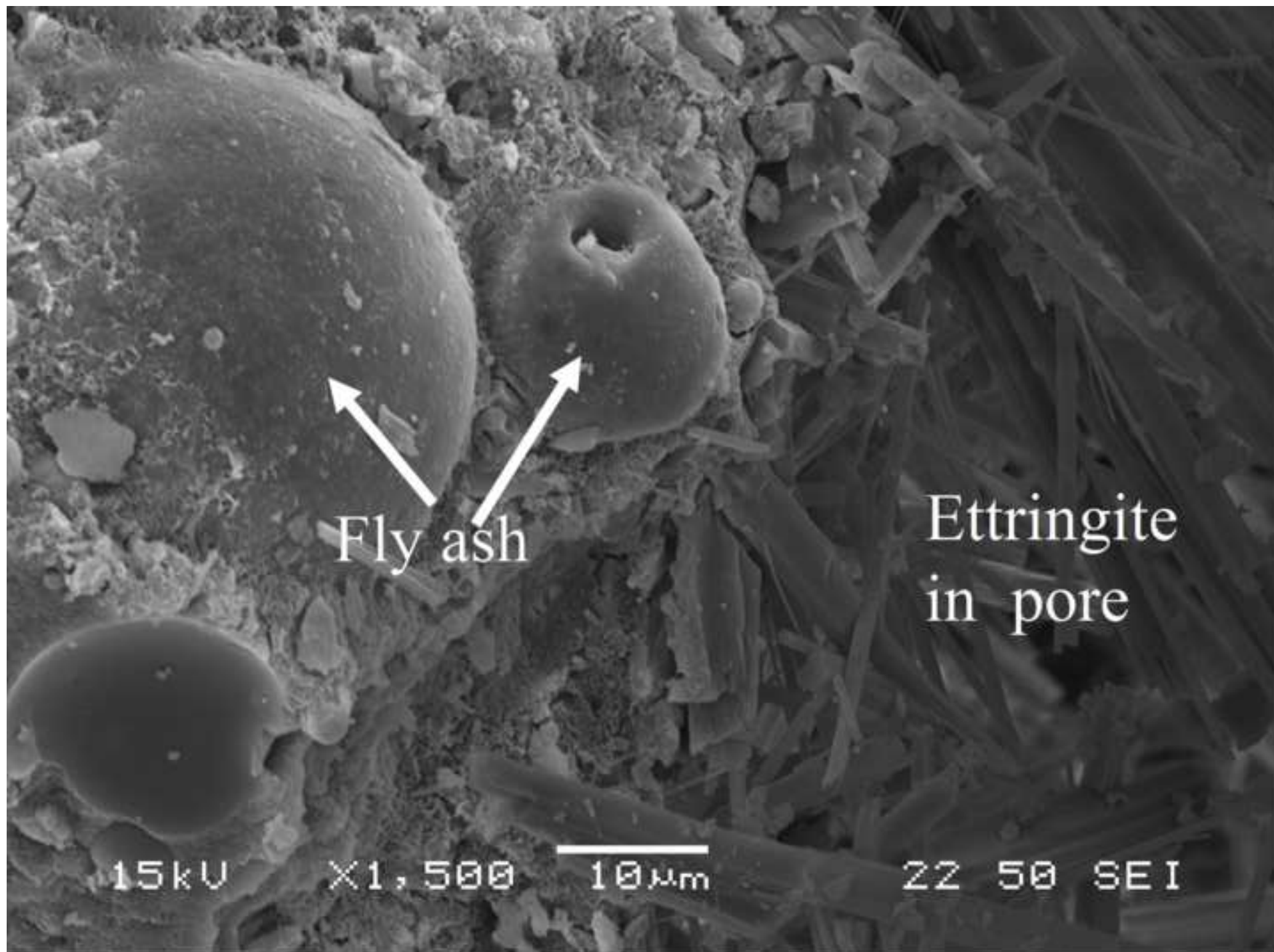
Figure_15
Click here to download high resolution image
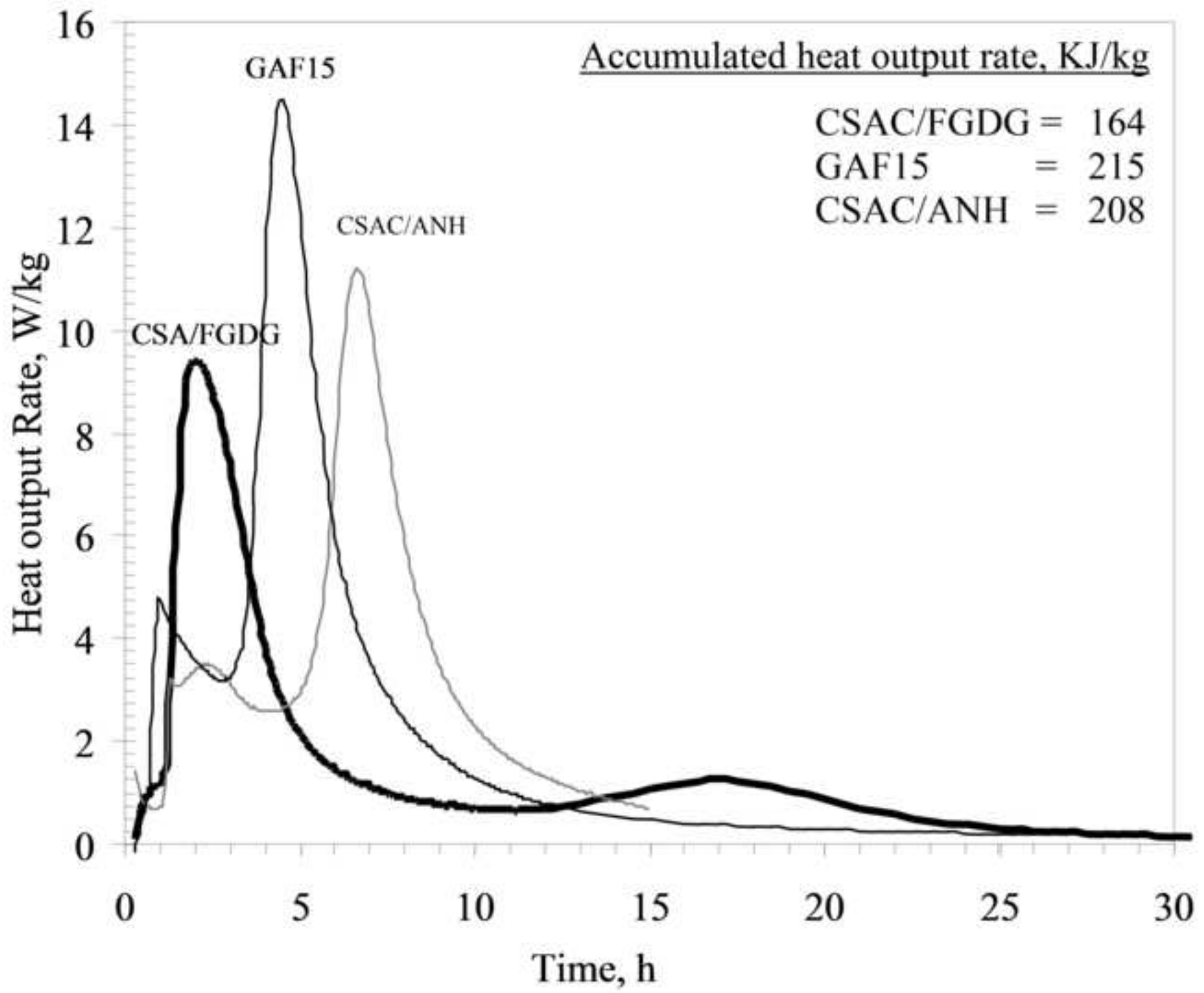
Figure_16
Click here to download high resolution image

Setting time, minutes